

Review

# Applications of Advanced Technologies in the Development of Urban Flood Models

Yuna Yan <sup>1</sup>, Na Zhang <sup>1,2,\*</sup> and Han Zhang <sup>1</sup><sup>1</sup> College of Resources and Environment, University of Chinese Academy of Sciences, Beijing 100049, China<sup>2</sup> Beijing Yanshan Earth Critical Zone National Research Station, University of Chinese Academy of Sciences, Beijing 101408, China

\* Correspondence: zhangna@ucas.ac.cn

**Abstract:** Over the past 10 years, urban floods have increased in frequency because of extreme rainfall events and urbanization development. To reduce the losses caused by floods, various urban flood models have been developed to realize urban flood early warning. Using CiteSpace software's co-citation analysis, this paper reviews the characteristics of different types of urban flood models and summarizes state-of-the-art technologies for flood model development. Artificial intelligence (AI) technology provides an innovative approach to the construction of data-driven models; nevertheless, developing an AI model coupled with flooding processes represents a worthwhile challenge. Big data (such as remote sensing, crowdsourcing geographic, and Internet of Things data), as well as spatial data management and analysis methods, provide critical data and data processing support for model construction, evaluation, and application. The further development of these models and technologies is expected to improve the accuracy and efficiency of urban flood simulations and provide support for the construction of a multi-scale distributed smart flood simulation system.

**Keywords:** artificial intelligence technology; remote sensing; crowdsourcing geographic data; Internet of Things; spatial data management and analysis; distributed smart flood simulation system



**Citation:** Yan, Y.; Zhang, N.; Zhang, H. Applications of Advanced Technologies in the Development of Urban Flood Models. *Water* **2023**, *15*, 622. <https://doi.org/10.3390/w15040622>

Academic Editors: Jorge Leandro and Mingfu Guan

Received: 18 December 2022

Revised: 1 February 2023

Accepted: 2 February 2023

Published: 5 February 2023



**Copyright:** © 2023 by the authors. Licensee MDPI, Basel, Switzerland. This article is an open access article distributed under the terms and conditions of the Creative Commons Attribution (CC BY) license (<https://creativecommons.org/licenses/by/4.0/>).

## 1. Introduction

In recent years, frequent extreme rainfall events have caused severe flooding worldwide. In addition, the rapid increase in impervious areas associated with urbanization has aggravated urban floods. For example, the peak flow of urban floods is several times or even dozens of times higher than that of natural rivers [1]. Frequent urban floods have seriously affected the normal functioning of cities. During and after rainstorms, rapidly accumulated floods cannot be discharged within a short time, which may have a significant impact on traffic, human lives, and even cause casualties. Given that urban areas have highly dense populations, numerous buildings, developed industries, and commerce activities, the impacts of floods are much more severe in urban areas than in natural areas. According to the Emergency Events Database, flooding is responsible for over one-third and more than half of global emergency event-related economic losses and fatalities, respectively [2]. For example, a flood in Queensland in September 2010 affected more than 200,000 people and led to a loss of \$2.38 billion [3]. A total of 641 out of 654 cities have been exposed to urban floods in China [4]. The '7.21' flash flood of Beijing in 2012 affected nearly 1.9 million people, caused a disaster area of 14,000 km<sup>2</sup>, and produced losses of approximately \$1.6 billion [5]. The extraordinary rainstorms and floods in Henan Province, China that took place on July 16, 2021 affected 150 counties, 1616 towns, and 1.47 million people and caused direct losses of \$17.96 billion [6]. Moreover, a large amount of pollutants is washed off during runoff periods and enters rivers and groundwater, which consequently degrades the water environment. To reduce disaster consequences while guaranteeing the normal functioning of cities, flooding prevention and mitigation measures must be formulated, and the timely warning of urban floods is an indispensable basis. Spatial assessments

of infrastructure flood exposure are a necessity for rational flood risk assessments, targeted mitigation measure implementation, and for ensuring local community preparedness [7]. To that end, large-scale assessments of flood-exposed areas and their spatial inequalities have attracted research attention [8].

Urban flood simulation is a generally used and valid approach for timely flood warning and spatial flooding assessments [1,9], and associated models are constantly evolving. The widely used models include the storm water management model (SWMM) [10–12], the MIKE FLOOD model [13], the InfoWorks ICM (integrated catchment management) model [14,15], and the Hydrologic Engineering Center’s hydrologic modeling system (HEC-HMS) and river analysis system (HEC-RAS) [16]. These models can simulate surface runoff and overflow processes, and the results can be used to derive rainstorm flood information. However, more accurate simulations are required to realize more reliable flood warning, including the refinement of inputs with higher temporal and spatial resolution; the collection, processing, management, and analysis of a large amount of multi-source spatially heterogeneous data; the finer demarcation of sub-catchments or land cover patches; the calibration and automatic adjustment of a variety of parameters; and more detailed descriptions of hydrological and hydrodynamic processes. Moreover, the actual flooding process is difficult to observe during severe rainstorms, and measured flooding data are not easily obtained from government departments or companies, which are issues that hinder the validation of modeled results.

The accuracy of flood model data for inputs and validation can be improved by applying advanced technologies, such as remote sensing [17], crowdsourcing geographic data, and Internet of Things (IoT) technologies [18]. However, a higher simulation accuracy generally implies a lower computational efficiency. Hence, models involving detailed processes at a fine spatiotemporal grain level are not suitable for urgent flood warning systems. Data-driven models based on artificial intelligence (AI) technology or models fused with AI can address this contradiction by ignoring or attenuating the interior mechanisms of hydrological and hydrodynamic processes and only if there is sufficient high-quality data. Geographic information systems (GIS) are integrated platforms that play an important role in data management, analysis, and simulation. In recent decades, GIS use has been well established, and Earth observation data have become increasingly available, which has increased the feasibility of large-scale evaluations at fine resolutions. Approaches and methods of spatial analysis are helpful for extracting multi-scale spatial information on input and output data and for linking multi-scale processes. In summary, these advanced technologies can be used at each level of model development, including constructing multi-scale flood models or fusing different models; obtaining, selecting, processing, managing, and analyzing model input variables and parameters; validating modeled flooding processes; and presenting spatial patterns of modeled flooding status.

This review first summarizes the characteristics of different types of main urban flood models. Approximately ten studies and review articles have already performed comparisons of different urban flood models [19–21]; therefore, this study focuses on the recent applications of advanced technologies in urban flood simulation and discusses insights into promising opportunities for future research.

## 2. Methods

The process of collecting and analyzing the literature consists of three steps. First, we selected “urban flood” and “model” as the key strings for the topic search. The literature published during 1980–2022 (up to March 9, 2022) was searched in the Web of Science (WOS). All publications containing either of these key strings in their abstracts, titles, or keywords were retrieved from the bibliography. We assumed that the publications in the WOS represented influential works capable of demonstrating the trends in the research field; however, the retrieved works did not cover all related studies, such as those in non-English languages. Second, using the co-citation analysis tool in CiteSpace software, 120 important publications with higher co-citation intensity were selected from

the bibliographic records. Moreover, some recently published articles were also reviewed. Finally, from these important publications, we extracted information related to urban flood models and advanced technology applications.

### 3. Descriptions of the Main Urban Flood Models

Urban flood models have been developed to understand various hydrological or hydrodynamic processes of floods in urban areas and to obtain flooding conditions, such as inundation area, flood depth, and volume.

The main simulated processes include surface runoff, surface convergence, pipe convergence, and flood inundation (Figure 1) [22,23]. Surface runoff is determined based on the amount of rain falling to the surface and the subtraction of the amount of evaporation from rain intercepted by the canopy, absorbed through infiltration, and detained in depressions [24]. The most commonly used methods for simulating surface runoff include the full storage runoff method, the infiltration curve subtraction method, the index deduction method, and the runoff coefficient method [25]. Surface convergence is the process of surface flow into drainage networks and rivers, and it is usually simulated using hydrological and hydrodynamic methods [26,27]. Hydrological methods include isochronal, linear, and nonlinear reservoir algorithms. Hydrodynamic methods are based on microscopic physical laws by numerically solving continuity and momentum equations. The most widely used method is the 2D shallow water equation. Pipe convergence refers to the confluence process of surface runoff after it enters rainwater pipe networks, and it is commonly simulated using the kinematic wave, diffusion wave, dynamic wave, instantaneous unit hydrograph, and Muskingum methods [28]. The flood inundation process describes the overflow of water in rivers or pipelines, and is mainly simulated using the 2D hydrodynamic method, the terrain submergence method, and the cellular automata method [29].

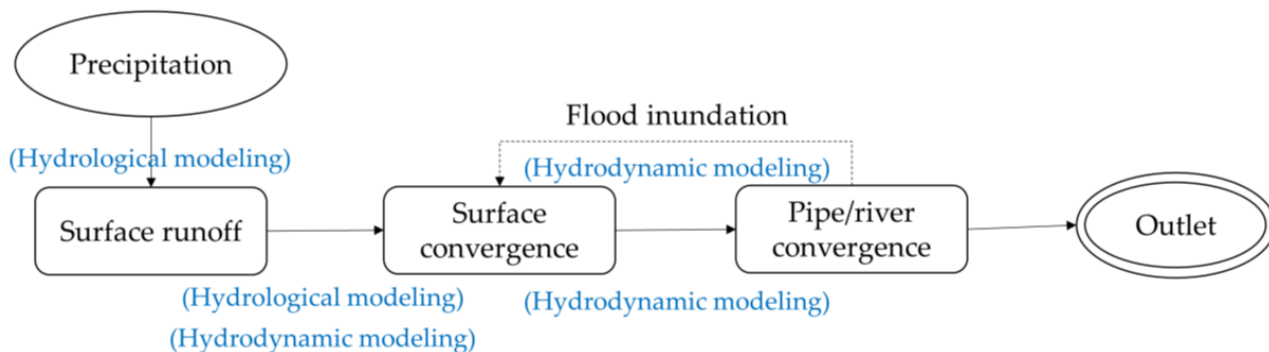


**Figure 1.** Urban flooding simulation processes (adapted from [30]). The simulations involve hydrological processes, from precipitation, to surface runoff and hydrodynamic processes, that generate flood inundation.

Distinct urban flood models involve different hydrological and hydrodynamic processes. Based on previous classifications [20,21,31], we summarized these models as simplified flood models, physical flood models, and data-driven models according to the complexity of the model structure, the described processes, and the amounts of required data (Figure 2). Simplified flood models require less input data, owing to their simple structure and relatively few model parameters. Physical flood models have the most complex structures and largest number of model parameters, and they require more data for parameter calibration and model validation. Data-driven models do not have complex structures but require massive data on the characteristics of flood events.

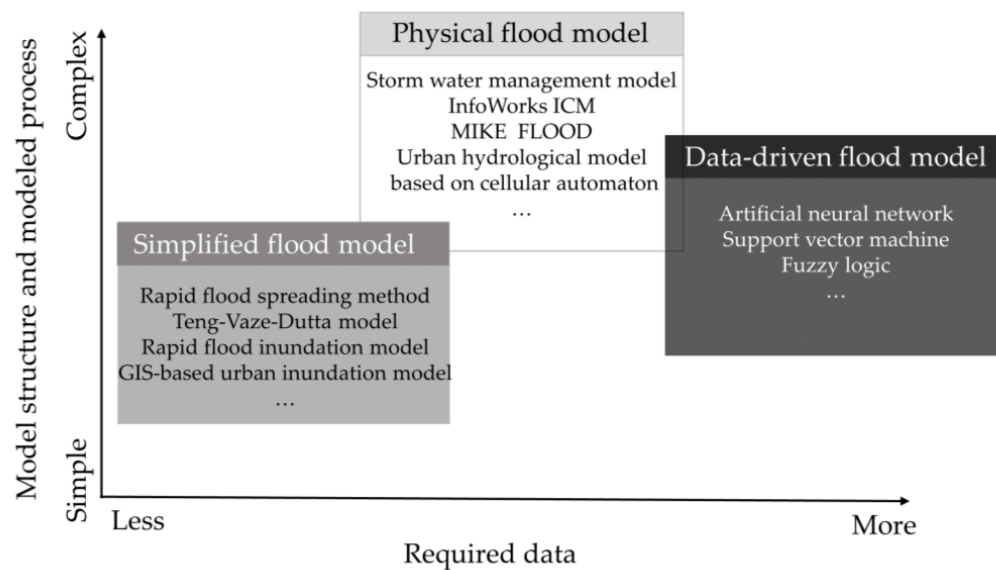


**Figure 2.** Classification and characteristics of the main urban flood models based on the complexity of the model structure and modeled processes and the amount of required data.

### 3.1. Simplified Flood Models

Simplified flood models can be regarded as gray-box models that do not clearly describe the internal laws of urban flooding. They have been widely used when the physical mechanisms of floods are unclear [32] and simulate flood processes by solving simplified equations (e.g., shallow water equations) that omit one or two acceleration terms [33]. The final or maximum flood range and related depth are obtained by solving the water balance equation.

These models have obvious advantages, such as reduced computational time. Jamali et al. developed a simplified model and showed that it could reduce the simulation time by two orders of magnitude when compared with MIKE FLOOD, although differences were observed in the simulated flood depth [33]. When the required simulation accuracy is not high or the situation is urgent, a simplified model can provide a stop-gap approach for rapid flood prediction.

### 3.2. Physical Flood Models

Compared to simplified flood models, physical flood models can be regarded as white-box models that describe the internal mechanisms of flood generation and are more suitable for the refined simulations of complex urban underlying surfaces.

Typical physical flood models include SWMM [10,34], MIKE FLOOD [35,36], InfoWorks ICM [15,37], and HEC-HMS/RAS [16,38]. Urban hydrological models have also been developed based on cellular automata, which we call UHCA models [39–41] (Figure 2). Most physical flood models use the catchment as the basic hydrological unit, whereas UHCA models use grid cells as units to achieve the fine division of underlying surfaces. Except for the SWMM, most physical flood models can simulate the flow of floods on a 2D surface. Moreover, some models include a pipe network module, some include a GIS module to achieve efficient processing of the driving variables and parameters, and some include a low-impact development (LID) module to describe local eco-hydrological processes in detail. The SWMM takes less time owing to more simplifications, and it may have lower simulation accuracy. By contrast, InfoWorks ICM and MIKE FLOOD can obtain more accurate surface flood distributions, although their calculation speeds are relatively low. The calculation speed and accuracy of the HEC-HMS/RAS model are relatively low [38]. UHCA models have the advantages of the above models and can simulate a flood event at the second to 10 min level [41]. They also present high accuracy based on the use of high-precision data at the grid cell scale and high efficiency based on the use of parallel

computing rules. Hence, UHCA models can support large-scale and high-precision spatial calculations in urban areas (Table 1).

**Table 1.** Comparisons of the main physical flood models.

Model	SWMM *	InfoWorks ICM *	MIKE FLOOD	HEC-HMS/RAS *	UHCA *
Basic unit	catchment	catchment	catchment	catchment	grid cell
Dimension	1D	2D	2D	2D	2D
GIS module	×	√	√	×	×
Pipe module	√	×	√	×	√ or ×
LID * module	√	×	imperfect	×	√ or ×
Calculation speed	****	***	**	*	****
Accuracy	**	***	****	**	*****
Open source	√	×	×	×	√ or ×

Note(s): \* SWMM, storm water management model; InfoWorks ICM, InfoWorks integrated catchment management model; HEC-HMS/RAS, Hydrologic Engineering Center's hydrologic modeling system and river analysis system; UHCA, urban hydrological models based on cellular automata; LID, low impact development. The larger number of the character of “\*\*” means the higher calculation speed or the higher accuracy.

Developing a hybrid model by utilizing the distinct advantages of different models or modules is a feasible and efficient approach. For example, we developed and validated a cellular automata-based distributed hydrological model for urban surface runoff (CADUSRM) [42], and then the simulated surface runoff was input into the pipe convergence module in SWMM for pipe overflow. Ultimately, the simulated overflow was input into a developed flood inundation module for the occurrence and expansion of inundation. This hybrid model has been validated in a small area and a large area using the measured and crowdsourced data.

These physical flood models describe the complex hydrological and hydrodynamic processes of floods in cities through physical laws formulated by differential equations, such as the Saint Venant, shallow water, and Boltzmann equations [43]. To simulate the temporal dynamics and spatial patterns of runoff and flood processes, these models generally require various data, such as topography, soil types, sewer conveyance networks, infiltration conditions, flow curves, and runoff parameters [43]. If these required data are difficult to obtain, it becomes impossible to use a physical model, especially for urban catchments with complex underlying surface conditions, boundary conditions, and intricate drainage systems. In addition, iterative calculations in simulations of urban runoff and flood processes require substantial time, and parallel computation in UHCA models requires adequate preparation for massive computing performance, which contradicts the short duration of urban flooding. All of these factors have greatly restricted the timely application of these models.

### 3.3. Data-Driven Flood Models

Data-driven flood models can be regarded as black box models without presenting the internal mechanism of flooding. These models have the most straightforward approach to forecasting the occurrence and magnitude of floods, which are based on historical data [20,21,31,44–49]. The black box nature of AI technology makes it a core algorithm for data-driven models.

Data-driven models exhibit good self-learning and continuous evolution capabilities [50]. In particular, they do not require an understanding of internal specific mechanisms and can avoid describing complicated hydrological and hydrodynamic processes. Data-driven flood models can automatically better extract flood features than simplified flood models. Moreover, they have a higher calculation efficiency and much lower requirements for flooding parameters than physical flood models. Therefore, data-driven flood models may provide rapid forecasts for urgent urban floods. However, these models require considerable historical data to train the simulation process and validate the simulation results.

To realize accurate prediction and control over an entire study area, flood models should contain more spatial elements; thus, spatially explicit models may be necessary [51]. Even if the model is not spatially explicit or developed for local sites or single sub-catchments, the spatial heterogeneous nature of flooding conditions and associated driving variables must be characterized. Obviously, both the development of spatial models and the identification of spatial patterns can benefit from emerging technological advances.

#### 4. Development of Urban Flood Models Using Advanced Technologies

The development of urban flood models requires a consideration of model construction, evaluation, and application. In addition to the model structure and algorithms, data issues penetrate throughout the process of model development.

##### 4.1. Model Construction

AI algorithms have been utilized in urban flood fields to develop data-driven models that can provide timely prediction of the imminent incidences of flash floods [52]. Many AI systems rely on machine learning methods, and deep learning is a new method for machine learning (Figure 3). The deep learning method analyzes and learns by establishing and simulating the neural network of the human brain. Compared to traditional machine learning methods, in which features are first manually extracted from data, deep learning methods can learn these features while training a large amount of data [53].

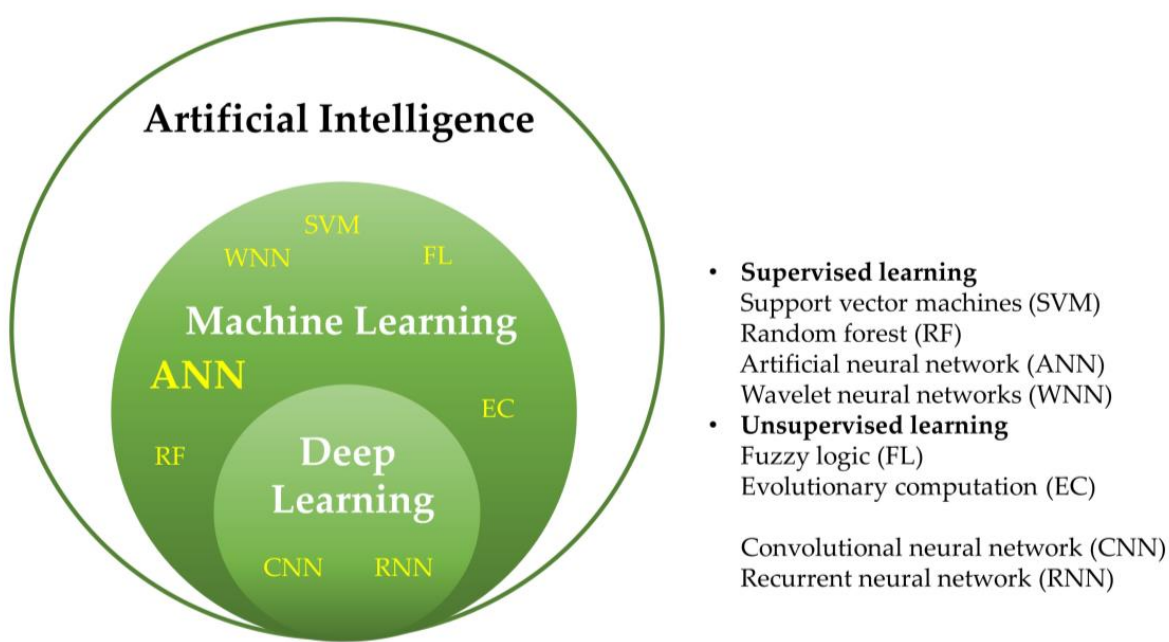


**Figure 3.** Categories of artificial intelligence algorithms that can be applied in urban flood simulations.

Common AI models involve three main layers: input, hidden, and output layers (Figure 4). The output layer contains data on flood variables, such as inundation area [54], flood volume [9], and flood depth. The input layer contains data on feature factors that may impact flood variables, such as precipitation [9], topography [55], normalized difference vegetation index (NDVI) [50], soil moisture, land use type (or imperviousness) [56], and urbanization level, which can be identified by correlation analysis. Although various input data can be provided to train a model, a systematic investigation should be considered to determine which inputs are optimal to predict flood variables [49]. AI algorithms and network structures are trained in one or multiple hidden layers to determine the appropriate weights that describe the relationships between the input and output variables. Flood data that are independent of those used for model training are used to validate the simulation results. After the model is validated to be reliable and accurate, model evaluations can be

conducted, including sensitivity analysis of the model parameters, uncertainty analysis of the simulation results, and comparisons with other models. Furthermore, the validated models can be used to provide flood warnings, flood risk assessments, and advice for landscape planning.

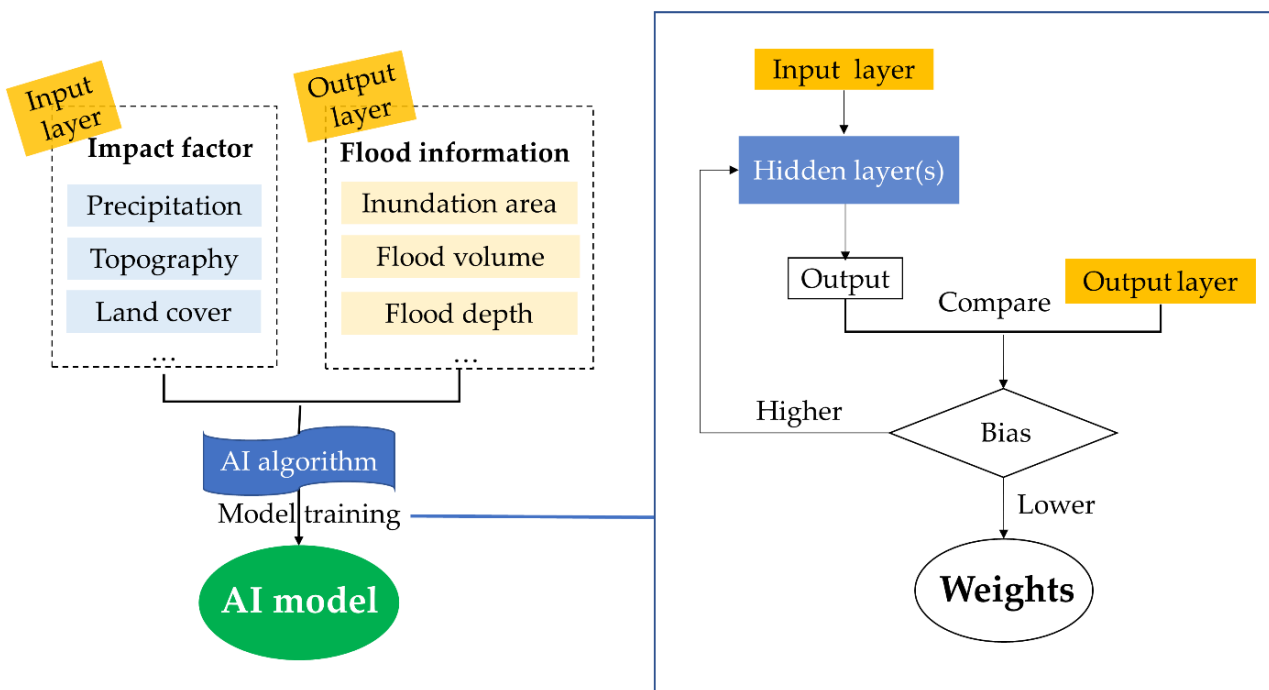


**Figure 4.** General flow chart for constructing an artificial intelligence model.

Over the last decade, a tremendous increase in the use of AI technologies has been observed for urban hydrological simulation, which has provided early warnings and real-time forecasts to decrease flood risks and losses [57]. AI algorithms have been used at single sites (1D) and achieved better results than traditional physical models. For example, Ke et al. used a rainfall threshold to differentiate flood events from non-flood events based on a support vector machine (SVM), which improved the accuracy of flood identification to 96.5% when applied to Shenzhen, China [58]. Tian et al. used a recurrent neural network for 1D flood runoff prediction, and the Nash coefficient was greater than 0.8 [59]. Furthermore, the prediction of a 2D flood inundation area and flood depth is more difficult, because there are many more feature factors and more complex nonlinear relationships between the input and output variables. To this end, exploratory studies have been conducted. For example, Berkahn et al. implemented an ensemble training approach and network growing algorithms for an artificial neural network (ANN) for 2D distributed maximum water level prediction in urban areas [47]. Chang et al. used a convolutional neural network to predict potential rainfall events from hyetograph feature parameters and to further estimate flood depth [52]. Hou et al. established a model that can rapidly estimate urban flood inundation based on machine learning algorithms (random forest and K-nearest neighbor) and showed that these algorithms can effectively improve the estimation accuracy; for example, the mean relative errors between the modeled and measured inundation area and flood depth values were less than 5%, and the mean relative errors between the modeled and measured flood volume values could be controlled to within 10% [60]. Moreover, AI-based systems have been developed. Ye et al. suggested an AI-driven platform for urban flood prevention and warning [61], and Goyal et al. created a system for real-time post-flood management using an ANN to analyze the areas affected by floods, and they found that this system was better than previous flood control systems [62].

The application of AI in urban flood simulations has greatly improved the efficiency and intelligence of estimations, as well as provided important support for the development of smart water cycle systems. AI algorithms can numerically formulate the nonlinearity of urban flood dynamics based solely on data. In addition, they can avoid iterative calculations of complex physical equations. Therefore, data-driven AI algorithms are promising tools for rapidly training and validating models.

However, the advantage of AI models also implies a disadvantage associated with a limitation. We cannot generate an explicit understanding of the underlying physical processes from either a data-driven AI model or its simulation results, which may lead to doubts in the model reliability, even if the simulation results have higher accuracy. Moreover, conflicts may occur between the simulation results and known physical principles [63]. To overcome this limitation, new AI theories and methods that couple data with a priori knowledge represent promising approaches [64]. For example, after the hydrological-related values modeled by physical models under various rainfall scenarios are validated, they can be used as training and test samples for an AI model. Bermúdez et al. used a hydrological model to generate discharge, which was input for SVM models with approximately 25,000 control points in an urban catchment for the output of the maximum flood depth and velocity [65]. Lin et al. generated a synthetic event database using the hydrological model LARSIM (large area runoff simulation model) [48] for discharge hydrographs and the HEC-RAS 2D hydrodynamic model for flood inundation map, and, then, these databases were used for training and validating an ANN. This is considered a loose coupling approach.

When the model is used over a large spatial extent, close coupling between a spatially distributed flood model and an AI algorithm becomes necessary. This type of coupling model has higher requirements for the training algorithms and network structures because of the complex nonlinear relationships between the spatial input and output variables that may exist at distinct scales. The structure of an AI flood model (such as the network topology and convolution core) can be adjusted according to the generation and evolution of spatially distributed flooding processes [64]. Moreover, prior knowledge can be used to constrain the range of model outputs to enhance the authenticity of simulation results. At present, the development of AI models driven by data that are guided and constrained by prior knowledge is still in the stage of theoretical exploration [66]. Although few related examples are available in the field of flooding, this idea has been applied in geosciences. For example, Chen and Zhang proposed a mechanism-mimicking AI network structure designed according to geomechanical equations [67].

In addition to AI algorithms, this type of coupling model has the requirements for the physical mechanisms that describe hydrological and hydrodynamics processes. There are certain uncertainties in the physical mechanisms. For example, the Saint Venant, shallow water, and Boltzmann equations generally used in physical models are more suitable for continuous processes on free surfaces [21]. For noncontinuous processes on a surface with large undulations or complex and heterogeneous land covers (typically in cities), there might be big errors. Although UHCA models can address this problem, our study showed that there is much room for the improvement of rules that describe intercellular water exchanges in multiple flow directions [42]. The incomplete laws and imperfect algorithms in numerical simulation and deep learning increase the uncertainties of simulation results.

#### 4.2. Data for Model Construction and Application

The construction of both pure data-driven models and data-driven models coupled with mechanisms require massive amounts of data for model training, and it also requires a large amount of data for model inputs and validation when a constructed model is applied over a large space. Therefore, collecting, processing, and identifying high-quality data have become major issues in both model construction, evaluation, and application.

In the era of big data, the amount of data related to urban flooding has sharply increased with the development of information collection technology. For instance, a large amount of meteorological data (4–5 PB) have been collected, with an annual increment of 1 PB, and frequent exchanges occur among countries worldwide [68]. Representative big data include crowdsourcing geographic data and IoT data, in addition to remote sensing and traditional site data (Figure 5). Various data have been used as inputs to provide meteorological data and flood-related data for urban flood simulation during both model training and application, and some can provide information for the calibration of parameters and the validation of modeled results. Model-predicted flood information (e.g., inundation area and flood depth) is generally communicated to mobile instruments or web users. Big data technology essentially unifies data from different sources and structures to provide support for urban flood simulations.

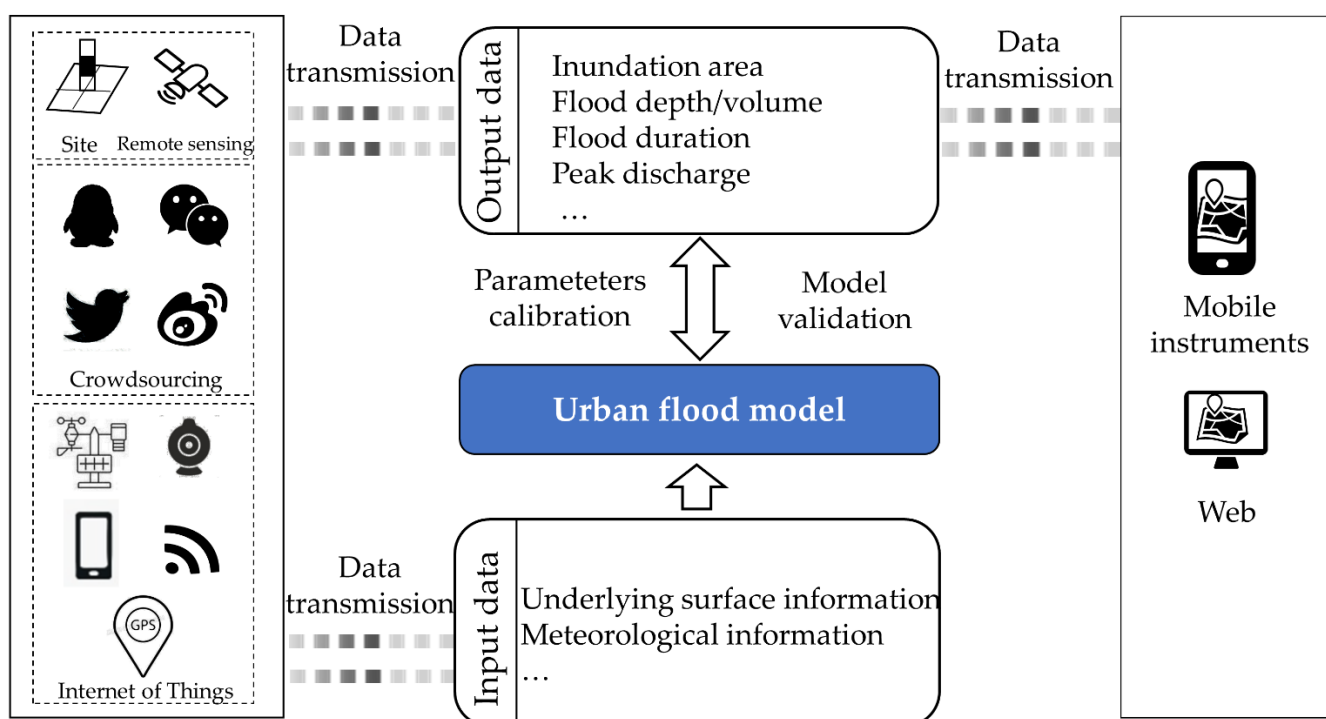


**Figure 5.** Big data technology involved in the construction, parameter calibration, validation, and application of urban flood models.

#### 4.2.1. Remote Sensing Data

Remote sensing technology has become increasingly significant in the field of flood simulation, especially with the continuous emergence of multi-platform, multi-temporal, and high-spatial-resolution remote sensing products. This technology can be used to detect broad-scale land surface data at a low cost and high efficiency, which may compensate for the shortcomings of traditional in situ measurements. Moreover, it can also provide information on underlying surfaces, meteorological factors, and water flows to develop and implement flood laws, although such technology is currently mainly applied in natural watersheds.

##### 1. Underlying Surface Information

In urban flood models, underlying surface information with an effect on floods mainly includes topographic and land surface characteristics (e.g., buildings and land cover) [69].

The depth and speed of floods are easily affected by urban micro-topographical characteristics. Thus, small topographic errors may lead to significantly distorted simulation results. The complex variation in microtopography in urban areas may involve various combinations of altitude differences, slopes, undulations, and overland flow widths, which can

generate nonlinear water flow processes [70]. For example, the altitude difference between two sites directly affects the water flow direction, which, thus, implies the expected position of the outlet within a sub-catchment and determines the discretization of sub-catchments. The combination of terrain undulation (concaveness/convexity of terrain) and slope affects the water flow speed and, thus, the water storage within a sub-catchment, which ultimately has an effect on runoff, convergence, and flooding [42]. Therefore, obtaining terrain data with a high spatial resolution is critical for revealing the flood flow mechanisms influenced by the terrain.

Currently, commonly used digital elevation model (DEM) data sources include the shuttle radar topography mission (SRTM, 30–90 m resolution), the advanced space-borne thermal emission and reflection radiometer (ASTER, 30 m resolution), and Google Earth (from multi-source data fusion and interpolation at approximately 7 m resolution) [71]. In addition, the latest remote sensing technologies, such as synthetic aperture radar interferometry (InSAR) and light detection and ranging (LiDAR), have further improved the accuracy and speed of terrain data acquisition. InSAR and LiDAR can provide terrain data with meter-level resolution over a large range. Fine LiDAR data are used to identify highly heterogeneous microtopography and building contours, which can facilitate the rapid development of high-spatial-resolution flood simulations [72,73]. However, this high-resolution data may not be necessary for a sub-catchment with small terrain undulations. Our studies showed that the modeled surface runoff processes for a sub-catchment without apparent depressions did not change significantly when the spatial grain size increased from 1 m to approximately half the sub-catchment area [42].

Land cover is another indispensable input data type when modeling runoff and flooding processes. Pervious and impervious covers have significantly different effects on overland flows, because they have different capacities for water retention, storage, absorption, and infiltration, which are determined by their physical characteristics (e.g., roughness, depression storage, and permeability), as well as biological and chemical attributes (e.g., plant utilization and soil absorption) [74]. Thus, the pervious or impervious area ratio is critical for the generation and dynamics of surface runoff and flooding. The spatial configuration among pervious covers, impervious covers, and outlets determines the overland flow routing and is also considered in some models, such as SWMM and MIKE FLOOD [75]. For plant cover, distinguishing herbs and shrubs from trees and determining their leaf areas are also necessary to better understand the effects of different vegetation types in mitigating flooding by more accurately simulating eco-hydrological processes, such as canopy interception of rainfall [76]. For hardened surfaces, different underlying surface materials (e.g., asphalt, cement, and brick) with different roughness values and permeabilities must be identified. Other land use types, especially those closely associated with human activities in urban areas, such as LID facilities, need to be identified because of their different eco-hydrological effects. The complexity and diversity of urban land cover and land use require data with a high spatial or spectral resolution to identify the types and materials of the underlying surface and to discretize sub-catchments. In some dynamic urban research, land use data with a high temporal resolution are also needed [77].

In the past few decades, remote sensing techniques have been used to obtain land cover and land use data through feature extraction and classification based on distinct electromagnetic wave information of the land surface objects. In contrast, hyperspectral remote sensing technology has greatly improved the ability to distinguish and recognize urban features, because it reduces the occurrence of phenomena in which different objects may have the same spectrum and the same object may have different spectra [78,79]. However, the spatial resolution of an image is generally low when its spectral resolution is high, which increases the difficulty of extracting and classifying complex features in urban areas. Generally, easily obtained high-spatial-resolution images are used as supplements to hyperspectral data. Globally, the mainstream remote sensing satellites with high spatial resolution include IKONOS, SPOT-5, the Earth Observation System, QuickBird, WorldView-1/2, Beijing-1, and Gaofen, and their spatial resolutions can reach the meter level [80].

## 2. Meteorological information

Meteorological data represent important inputs for urban flood models. With the development of remote sensing technology, many meteorological-related data, such as rainfall [81], evapotranspiration [82], and soil moisture [83,84], can be rapidly quantified using retrieval algorithms [85,86].

Precipitation observations based on remote sensing images represent the most effective method for obtaining spatial and temporal distribution characteristics and changes in urban rainfall. Satellite and fusion precipitation products have been widely used in urban flood simulations [87]. Satellite precipitation information primarily depends on the radiation characteristics of clouds in the atmosphere acquired from onboard sensors [88]. The radiation characteristics of clouds are directly related to the state parameters of the cloud layer, such as the cloud layer height and thickness, cloud top temperature, and cloud expansion rate. These parameters can be characterized using brightness temperature data obtained from sensors. At present, the cloud index and cloud life history methods are widely used to retrieve precipitation data based on the radiation characteristics of the cloud layer from visible/infrared images [89]. A precipitation calculation method based on statistical data and cloud radiation models was established for the retrieval of microwave observations [90].

Various satellite precipitation products have been produced, including tropical rainfall measuring mission (TRMM) multisatellite precipitation analysis (TMPA,  $0.25^\circ$ , 3 h), global satellite mapping for precipitation (GSMAP,  $0.1^\circ$ , 30 min–1 day), and integrated multisatellite retrievals for global precipitation measurement (IMERG,  $0.1^\circ$ , 30 min). These products can provide precipitation data with a wide variety of spatial and temporal resolutions for urban flood simulations. Their application in urban flood simulations have provided useful insights regarding the temporal evolution and spatial variation of the precipitation [91–94]. However, all satellite precipitation products failed to provide accurate rainfall records [92]. In general, these products have large systematic errors and random errors, which are affected by atmospheric attenuation, sensor performance, spatial resolution, and inversion algorithms [95]. In particular, IMERG data cannot reproduce local scale extreme precipitation, with an error of more than 70 mm, because of their coarse spatial resolution. Compared to satellite data, ground data have higher accuracy, and coupling with ground weather station data is a critical approach to obtain high-accuracy precipitation products. For example, the hourly precipitation grid dataset issued by the China Meteorological Data Service Center was coupled with CMORPH precipitation products based on data from the automatic weather stations from over all of China. However, these products cannot meet the requirement for the simulation of rapidly occurring and changing flash flood processes because of their low temporal resolution [91]. Given that ground weather stations and weather radar can provide the massive precipitation data continuously measured at minute or second levels, some studies developed the methods of fusing satellite data with ground data to generate precipitation products that can have a spatial resolution of 1 km and temporal resolution of 6 min under ideal conditions [95].

Evapotranspiration represents the water flux that diffuses from the endothermic phase change of surface water and vegetation water to the atmosphere, and it includes vegetation transpiration, soil evaporation, and canopy interception evaporation. Evapotranspiration may be ignored during rainstorms. However, it can greatly affect the water cycle and the ultimate soil water condition of an ecosystem before rainfall, which then influences infiltration, surface runoff, and flood genesis during rainfall. In urban areas, land use changes from permeable and moist natural surfaces (e.g., soil and vegetation) to large areas of impervious artificial surfaces (e.g., roads and buildings) fundamentally influence the thermodynamics, water circulation, and aerodynamic characteristics of the underlying surface and, thus, have direct consequences on surface evaporation and vegetation transpiration [96]. Currently, remote-sensing sensors cannot directly observe evapotranspiration and mainly measure surface parameters that are closely related to evapotranspiration, such

as surface temperature, specific emissivity, surface type, surface albedo, vegetation index, and vegetation coverage. These parameters can be used to estimate evapotranspiration.

Typical evapotranspiration products include the global evapotranspiration product MOD16, which is based on the moderate-resolution imaging spectrometer (MODIS), on global evapotranspiration products based on the advanced very high-resolution radiometer, and on global land evaporation Amsterdam model products. However, continuous evapotranspiration is difficult to estimate in space and time because of the transient nature of remote sensing images and cloud interference.

Soil water conditions can determine the water exchange between the atmosphere and land surface. Hence, soil moisture is an important parameter or an initial variable in flood models. Soil moisture can be retrieved from remote sensing images based on the spectral reflectance or emission characteristics of the soil and vegetation. For example, soil moisture estimates from the temperature vegetation dryness index rely on the land surface temperature and vegetation index, which can be easily retrieved from thermal infrared and visible near-infrared spectrum images, respectively [97]. Soil moisture estimates from soil thermal inertia depend on land surface albedo and the diurnal temperature range of topsoil, which can be retrieved from the multispectral reflectance and thermal infrared emissivity of topsoil at different times, respectively [98]. Some soil moisture estimates are retrieved from the brightness temperature obtained from microwave remote sensing images [99].

Existing soil moisture remote sensing products include essential climate-variable soil moisture ( $0.25^{\circ}$ ), soil moisture and ocean salinity (25 km), advanced microwave scanning radiometer 2 (25 km), and soil moisture active/passive detection satellite products (36 km) [100]. Although great progress has been made in the remote sensing inversion of soil moisture, many aspects need to be strengthened. For example, existing soil moisture data mainly represent moisture information of the top soil layer (usually 0–20 cm), which has limited applications in eco-hydrology studies, because the roots of most plants (especially trees) can reach far below the top layer [101]. In particular, current soil moisture data have low spatial resolutions and, thus, have limited applications in urban flood models. The development of future soil moisture inversion methods based on physical principles will be challenging because of the high number of factors (such as soil physical and chemical properties) that may affect soil moisture and the limited number of parameters that can be retrieved from remote sensing data under the current technical situation.

### 3. Flood information

Remote sensing technology has been widely used to identify water bodies (including floods) since the late 1970s, especially through the Earth Resources Technology Satellite and Landsat series [102]. Floods were identified based on the spectral characteristics of water compared with other land cover types. Flood information (range, depth, and duration) was extracted from the electromagnetic spectrum reflected by water to realize the dynamic monitoring of flood processes. This information can be used as samples for training urban flood models, calibrating parameters, validating simulated flood range or depth, and assimilating models [103].

Different types of remote sensing data have different advantages and limitations for identifying floods (Table 2). Optical remote sensing data have a large range of spatial and temporal resolutions and, thus, can meet the requirements for identifying flood range, depth, and duration at different scales. For example, the Gaofen-2 satellite data have a spatial resolution finer than 10 m, and the WorldView commercial satellite data even reach the submeter level. MODIS data can capture the dynamic process of water inundation during floods well because of their prominent advantages in high temporal resolution (0.5 d), high spatial resolution (250 m), and wide spectral range (0.4–14  $\mu\text{m}$ ) [104]. However, optical sensors are easily affected by clouds and weather, and obtaining effective data during flood events is difficult due to overcasting [105].

**Table 2.** Application of different types of remote sensing data to flood information identification for urban flood models.

Remote Sensing Data Type (Temporal and Spatial Resolution)	Flood Information	Characteristic	Satellite/Sensor
Optical data (0.5–26 days, <500 m)	Flood range Flood depth Flood duration	Vulnerable to clouds and weather	MODIS * Landsat TM *
Passive microwave data (twice a day, 10–70 km)	Flood range Flood duration	Less affected by weather; low spatial resolution; high temporal resolution	AMSR-E * TRMM/TMI * SSM/I * TerraSAR-X *
Active microwave data (14–28 days, 1–10 m)	Flood range Flood depth	Unaffected by weather; high spatial resolution; low temporal resolution	COSMO-SkyMed * ALOS *-2 Sentinel-1

Note(s): \* MODIS, moderate resolution imaging spectroradiometer; TM, thematic mapper; AMSR-E, advanced microwave scanning radiometer for the Earth Observation System; TRMM, tropical rainfall measurement mission; TMI, TRMM microwave imager; SSM/I, special sensor microwave imager; TerraSAR-X, terra synthetic aperture radar-X; COSMO-SkyMed, constellation of small satellites for Mediterranean basin observation-SkyMed; ALOS, advanced land observation satellite phased array L-band synthetic aperture radar.

Passive microwaves can penetrate clouds or vegetation and are less affected by weather conditions or land cover (Table 2). Passive microwave remote sensing sensors have a short revisit period, and their observation frequency can reach twice a day over most parts of the world; thus, they are suitable for monitoring broad-scale flood processes and ranges. Brakenridge et al. demonstrated that electromagnetic radiation reflected or emitted from the surface of floods (water) and land was very easy to distinguish when the band frequency of the horizontal polarization of the sensor was 36.5 GHz or 37 GHz [106]. However, passive microwave systems are rarely used alone to extract urban flood information because of the coarse spatial resolution of the data [107]. In contrast, active microwave systems have a high spatial resolution (1–10 m); thus, more accurate flood range and depth information can be obtained. Microwaves transmitted from such sensors can penetrate cloud cover, haze, and dust, regardless of the weather conditions, which means that flood events can be observed during the day and night [108,109]. Studies have developed automated flood detection algorithms or systems based on synthetic aperture radar (SAR) images. However, SAR may not be able to observe most of the land surface in urban areas with high buildings or tall trees because of its side-viewing nature, as well as the corner reflection that frequently appears for urban buildings with a rectangular surface structure [107,110].

The use of satellite remote sensing technology in flood monitoring and disaster emergency response is limited because of the transient transit time of satellites [111]. Unmanned aerial vehicle (UAV) technology is a new emerging technology that can compensate for this limitation. UAVs capable of carrying different sensors have become an important means of monitoring flood disasters over the past 10 years, because UAV surveys are flexible and convenient and can generate high-precision (submeter level) data [112]. Feng et al. used a UAV carrying an RGB digital camera to obtain optical images and monitor serious urban waterlogging in Yuyao, Zhejiang Province, China [113]. Researchers have also used UAVs carrying LiDAR (mainly composed of a global position system, an inertial measurement unit, and digital cameras) to reconstruct high-precision 3D models and DEMs, and they also combined UAVs with GIS spatial analysis technology to extract flood range data and assess flood risk [114]. In addition, the simultaneous localization and mapping (SLAM) technique with LiDAR equipment can quickly reconstruct the real-time surrounding scenes without time and place limitations; thus, it can obtain more precise flood-related data [115].

#### 4.2.2. Crowdsourcing Geographic Data

Crowdsourcing geographic data refer to open geographic data obtained by a large number of voluntary nonprofessionals and professionals and provided to the public in the form of text, pictures, and videos via the Internet (Figure 5) [116]. In current society, the public can play an unexpected role in the issue of real-time flood information, which increases the data size considerably.

Crowdsourced data are a type of unstructured data that belong to natural language text. Flood information extraction from crowdsourced data mainly rely on natural language processing, which is a type of AI algorithm. Fohringer et al. were the first to manually derive flood inundation area maps from social media posts on Twitter [117]. Li et al. used flood-related text information released on Sina Weibo to monitor rainstorm events in Wuhan and Shenzhen, China [118]. In addition to monitoring and presenting the current flood occurrence, these data may be used to validate the simulated flood situations and further develop a model with high reliability and accuracy [21]. Furthermore, the vulnerability to urban flood disasters or the risk of urban flooding can be assessed based on real-time crowdsourcing data [119].

#### 4.2.3. Internet of Things Data

IoT refers to a network that combines various sensors, such as infrared sensors, laser scanners, and global positioning systems, via the Internet or telecommunications networks [120]. In the field of flood studies, common IoT devices include wireless sensors, cameras, mobile phones, and automatic weather stations (Figure 5). They are usually located at specific locations, such as water-prone road sections, low-lying areas, underpasses of overpasses, and tunnels. By using these devices, the network can automatically identify, locate, track, and monitor real-time flood events [121], from which we can generate a large amount of continuous flood-related data (such as rainfall, flood flow speed, and flood depth) that can be used to construct or evaluate urban flood models. For example, an electronic water gauge can accurately monitor the dynamics of flood depth on a road at a minute level. The entire process of surface flooding and receding water in waterlogging events can be obtained from video surveillance systems; then, flood inundation information can be retrieved using computer image recognition technology. Based on the aforementioned technologies, high-definition cameras can detect real-time floods within a few seconds [117,122].

IoT systems are suitable for the early forecasting of urgent events, such as urban floods, because they can efficiently collect, manage, analyze, and share real-time data. Imminent rainstorm events can be predicted from the current meteorological conditions monitored by an IoT system and can then be used as inputs to predict the range and intensity of potential waterlogging through urban flood models. Subsequently, the IoT system can issue this information to the public via the Internet.

Hyper-resolution monitoring of urban floods that relies on crowdsourced geographic data and IoT data can supplement the deficiencies in traditional urban flood data and be expected to reveal more phenomena. However, the current application of these big data methods in urban flood simulation is limited. First, collecting a large amount of data is difficult because of the protection of users' personal privacy or intellectual property and the inability to deploy IoT devices over an entire urban area. Second, processing these big data requires a considerable amount of time. There are considerable redundancies and noise contained within these big data, and considerable data cleaning work is required, including checking the credibility of information and evaluating the uncertainty of flood location and depth [123]. Data cleaning relies on more advanced cloud computing technology for data resources and a more comprehensive big data computing framework for algorithm support.

#### 4.3. Spatial Data Management and Analysis

Although current advanced technologies have provided rich data for urban flood simulations, they have also introduced new challenges. First, rapid increases in various high-resolution data necessitate strict requirements for high-performance data processing, storage, and management. Second, approaches for fusing massive multi-source data and forming a comprehensive basic database should be developed. Most critically, the data obtained at multiple spatial and temporal levels also creates issues related to scaling, such as determining the relationships that occur between adjacent-scale or cross-scale data or information. Tackling these challenges requires more effective spatial data management and analytical methods.

##### 4.3.1. Spatial Data Platform

GIS has been widely used in flood simulations to provide spatial data management functions. More importantly, given that most urban flood models cannot express the spatial distribution of floods, the strong spatial analysis capabilities of GIS become indispensable.

Basic data analysis tools in GIS can be used to calculate the various parameters required for urban flood models. For example, hydrological analysis tools (e.g., basin, flow direction, and flow accumulation in ArcGIS software) have been used to determine the flow direction and water outlets in a sub-catchment using DEM data, based on which the sub-catchments become discretized [124]. The 3D analyst tool in ArcGIS has been used to calculate various parameters, such as the average slope of a sub-catchment. Zonal statistics in ArcGIS have been used to calculate the sub-catchment area and the pervious to impervious surface ratio based on land use data [125]. By using the topology function in ArcGIS, a drainage pipe network layout that represents the actual situation can be established, which is crucial for improving the simulation accuracy of pipe convergence processes [126]. Based on these tools, ModelBuilder programming techniques in ArcGIS can be used to develop automatic workflows of calculation processes, which can greatly improve the efficiency of processing data [124].

GIS can also provide a platform that integrates different technologies or models, such as spatial information technology, big data technology, AI technology, and hydrological models, to build an integrated urban flood information system. Jing et al. developed a model based on 2D unsteady flow theory using the ArcView software platform to construct a rainstorm and waterlogging monitoring and early warning system in Harbin, Heilongjiang Province, China [127]. Wang et al. used 1D open channel unsteady flow and 2D unsteady flow equations, combined with real-time rainfall monitoring data from regional automatic stations, to refine precipitation forecasts, as well as construct a dynamic forecast and early warning system on the Meteo GIS platform for urban waterlogging management in Langfang, Hebei Province, China [128]. Urban flood models have also been developed based on GIS platforms, such as MIKE Urban, InfoWorks ICM, and Digital Water DS. These platforms can convey detailed flood physical mechanisms, have fast processing capabilities for spatially distributed data, and present efficient modeling capabilities. Some studies mixed AI models and GIS analysis to extrapolate local forecasts to flooded areas at sub-catchment scales [129].

Future research will mainly focus on supporting real-time data formats [130], and 3D GIS will become a support platform for ensuring the accuracy and credibility of flood simulations [131]. Such research has considerable room for improvement.

##### 4.3.2. Spatial Data Analysis

Spatial analysis methods (especially spatial statistics methods) can play indispensable roles in determining suitable data inputs, in analyzing the spatial patterns of simulated flooding processes, in linking the patterns and processes among different scales, and in developing multi-scale distributed flood models.

The selection of spatial data depends mainly on the research purpose, scale of discretized catchments, and average size of historical inundation areas [132]. If we are con-

cerned only with large inundation areas in a large region, then coarse-resolution data and catchments are practicable. In contrast, if we are concerned with all the inundation areas regardless of their sizes or depths, then the fine-resolution data must be selected to identify catchments at a fine scale. Regardless of the type of concern, the spatial grain size of the data should be smaller than the average size of the inundated patches [133]. Thus, a method for determining the average patch size before performing spatial data selection is required. The average size of inundated patches (and their connectivity, proximity, isolation, aggregation, and dispersion) can be calculated using spatial pattern analysis software, such as Fragstats 4.2 [134], based on a generated raster image with various patch types. For a large and spatially complicated urban area, some spatial statistical methods (such as lacunarity index, spatial autocorrelation analysis, and scale variance analysis or scale variance analysis coupled with Moran's  $I$  scalogram) can help identify the average patch size [135,136].

The identification of multi-scale spatial patterns of flood-related variables (such as rainfall, soil moisture, evapotranspiration, and surface runoff) relies on spatial statistical methods. In addition to the methods mentioned above, which are used for patch-type data, wavelet analysis is widely used for quantitative variables. From the spatial statistical analysis, we may determine the nested hierarchical structure of these variables across scale domains in a large range, such as the small flooding aggregation occurring at local sites, medium aggregation covering multiple land covers, and large aggregation across adjacent sub-catchments. These spatial statistical methods can also identify whether a variable is spatially random, uniform, aggregated, or dispersed within each scale domain, as well as whether the two variables have a spatially positive or negative association. Within a limited range or scale domain, if the spatial pattern analysis shows that a variable presents a fractal structure rather than a hierarchical structure, then the complex flooding processes can be dealt with in a simple way based on power laws [137].

The multi-scale spatial pattern analysis of inundated patches and flood-related variables can help us not only explore the spatial patterns of patches and variables and their associations with hydrological processes within each scale domain, but also explore the pattern–process relationships across scales. Thus, spatial pattern analysis is the basis for developing a multi-scale distributed flood model across cell (or site), patch, sub-catchment (or catchment), and landscape (or region) scales [40,137]. If water flow interactions among cells are fully comprehended, then upscaling from cells to patches can be realized, and if water flow routings among adjacent patches are determined, then hydrological processes can be intrinsically upscaled from patches to sub-catchments or catchments [138]. We developed CA-DUSR, a cellular automata-based distributed hydrological model for urban surface runoff, in which the nonlinear reservoir algorithm was improved and combined with a weighting system to simulate surface runoff processes. We assumed that each cell interacted with other cells in its neighborhood via local surface water exchange rules. Such rules realize the upscaling of runoff, first from cells to their neighborhoods, and then from cell neighborhoods to their distinct nearest outlets. Ultimately, runoff converged to multiple outlets is lumped to a sub-catchment [42]. The whole upscaling is realized within the bottom-up simulation framework of cellular automata. The similar upscaling approach can be implemented when simulating the spatial expansion of water overflowed from pipe network nodes to their nearest neighborhoods and then to farther surroundings. More heuristic simulation approaches or sophisticated spatial technologies are required for future model development, which represents one of the most rewarding challenges.

#### 4.3.3. Uncertainty in Spatial Analysis

Although advanced technologies have facilitated flood model development, uncertainties exist in the spatial analysis methods for such models. Original data have errors, and estimated data have uncertainties [19]. For example, fine urban meteorological data and underlying surface parameters (e.g., depression storage, Manning's roughness coefficient, and soil texture) are mainly obtained from local ground stations and sample sites.

Uncertainties always occur when such data are spatially extrapolated to a large area, due to insufficient sample density and imperfect upscaling methods [138]. When multiple data with different types and sources are input to a flood model, data transformation to unified formats (e.g., the same resolution and geographical project) will inevitably produce deviations. Scale effect is another source of uncertainty for model outputs. Different spatiotemporal grains for the same variables or parameters may generate great discrepancies in simulated runoff and flood processes; for example, our study showed that increasing temporal grains can result in aliasing in hydrographs [42]. In these cases, the uncertainties of model outputs over a space can be estimated based on the statistical distributions of input data (and correlations between inputs) from their actual values or generated random values that conform to their statistical characteristics.

In addition, although certain technologies and approaches can theoretically be used to obtain the information on flood inundation range and depth, there might be still many places and times for which the information has not been covered. Such cases will make model validation difficult and uncertainty evaluations incomplete, especially for small flooded sites.

## 5. Conclusions

Urban flood models can be classified into three categories: simplified, physical, and data-driven. With the application of advanced technologies in flood models, the simulation accuracy and efficiency have improved markedly, thus providing support for the establishment of a smart and integrated model framework for urban floods.

Although a perfect urban flood model has not yet been developed, the advantages of distinct models can be combined to produce an optimal model. The designed perfect model framework should be a multi-scale distributed smart simulation system that considers cells as the basic units and supports simulations within and across distinct scales, such as cells, patches, sub-catchments, and catchments.

The optimal system involves three main parts: inputs, models (algorithms, functions or rules), and outputs. For model input variables and parameters, remote sensing, crowdsourcing geographic data, and IoT big data technologies and methods that have been sufficiently developed and improved should be considered via the spatial data management functions of GIS platforms. By using image processing software and 3D GIS technologies, the synthesis and presentation of real-time and authentic flooding maps should be a critical output part of systems for the early warning and control of floods.

Regarding the model, the expected models should integrate two types of general strategies that have separate requirements for flood simulation. The first general strategy focuses on simulation accuracy. For accuracy, modules associated with eco-hydrological and hydrodynamic processes at multiple scales, such as overland flow and inundation at the cell or local scale, runoff generation and confluence at patch-scale LID facilities, and overflow in pipe networks at the sub-catchment scale, should be considered and combined into the system using a common GIS platform. The modules should be continuously updated using the developed mechanisms. The second general strategy focuses on simulation efficiency. For efficiency, AI models that are trained using advanced algorithms based on a large amount of meteorological, topographic, land cover, and flood data are required. Given that we must simultaneously address the issues of simulation accuracy and efficiency during urgent urban waterlogging, the expected models should not be completely mechanism models or completely non-mechanism (or statistical) models; rather, they should effectively couple mechanism and non-mechanism models.

Although many advanced spatial technologies have been developed for the construction of the expected multi-scale distributed smart simulation system, challenges remain. The most difficult task is to determine the scaling laws of eco-hydrological and hydrodynamic processes based on the spatial pattern characteristics of processes and pattern–process relationships across scales. Resolving these issues will not only require advanced methods in spatial analysis, but will also require an understanding of the dynamics and mechanisms

at multiple scales. The second most difficult task is to develop models that can couple calculations driven by flooding processes with AI algorithms that are driven by data to realize high simulation accuracy and efficiency.

We suggest that a multi-scale distributed smart simulation system will provide more accurate flood information in a highly efficient manner, and such characteristics will be essential for the wide application of such systems for the early warning and control of floods.

**Author Contributions:** Funding acquisition, N.Z.; Writing—original draft, Y.Y. and N.Z.; Writing—review and editing, N.Z. and H.Z. All authors have read and agreed to the published version of the manuscript.

**Funding:** This research was supported by the Beijing Natural Science Foundation [8181001] and the Special Fund for Scientific Research Cooperation between Colleges and Institutes of the University of Chinese Academy of Sciences [Y65201NY00].

**Institutional Review Board Statement:** Not applicable.

**Informed Consent Statement:** Not applicable.

**Data Availability Statement:** Data will be made available upon request.

**Conflicts of Interest:** No potential conflict of interest was reported by the authors.

## References

- Chen, G.-Z.; Hou, J.-M.; Zhou, N.; Yang, S.-X.; Tong, Y.; Su, F.; Huang, L.; Bi, X. High-resolution urban flood forecasting by using a coupled atmospheric and hydrodynamic flood models. *Front. Earth Sci.* **2020**, *8*, 545612. [[CrossRef](#)]
- EM-DAT: The International Disaster Database. 2018. Available online: <http://www.emdat.be> (accessed on 18 December 2022).
- Carbone, D.; Hanson, J. Floods: 10 of the deadliest in Australian history. Australian Geographic. 8 March 2012. Available online: <https://www.australiangeographic.com.au/topics/history-culture/2012/03/australias-worst-floods/> (accessed on 18 December 2022).
- Task Force on Urban Flooding Problem and Solution Investigation (TFUFPSI). China's urban flooding program and solution. *China Floods Droughts Prot.* **2014**, *24*, 65. (In Chinese)
- Qiu, J. Urbanization contributed to Beijing storms. *Nature* **2012**, *10*, 11086. [[CrossRef](#)]
- Ye, M.-H.; Chen, K. Urban catastrophe risk: Meteorological characteristics, loss status and optimization of management countermeasures: Taking Zhengzhou "7.20" heavy rainstorm and Typhoon "Fireworks" as an example. *Shanghai Insur.* **2021**, *8*, 18–22.
- Stefanidis, S.; Alexandridis, V.; Theodoridou, T. Flood exposure of residential areas and infrastructure in Greece. *Hydrology* **2022**, *9*, 145. [[CrossRef](#)]
- Koks, E.E.; van Ginkel, K.C.H.; van Marle, M.J.E.; Lemnitzer, A. Brief communication: Critical infrastructure impacts of the 2021 mid-July Western European flood event. *Nat. Hazards Earth Syst. Sci.* **2022**, *22*, 3831–3838. [[CrossRef](#)]
- Contreras, M.T.; Gironás, J.; Escauriaza, C. Forecasting flood hazards in real time: A surrogate model for hydrometeorological events in an Andean Watershed. *Nat. Hazards Earth Syst. Sci.* **2020**, *20*, 3261–3277. [[CrossRef](#)]
- Agarwal, S.; Kumar, S. Urban flood modeling using SWMM for historical and future extreme rainfall events under climate change scenario. *Indian J. Ecol.* **2020**, *47*(11), 48–53.
- Rossman, L.A.; Huber, W.C. Hydrology. In *Storm Water Management Model Reference Manual*; EPA/600/R-15/162A; United States Environmental Protection Agency: Cincinnati, OH, USA, 2016; Volume 1.
- Rossman, L.A.; Dickinson, R.E.; Schade, T.; Chan, C.C.; Burgess, E.; Sullivan, D.; Lai, F.H. SWMM 5—The next generation of EPA's storm water management model. *J. Water Manag. Model.* **2004**, *12*, 339–358. [[CrossRef](#)]
- Anni, A.H.; Cohen, S.; Praskiewicz, S. Sensitivity of urban flood simulations to stormwater infrastructure and soil infiltration. *J. Hydrol.* **2020**, *588*, 125028. [[CrossRef](#)]
- Wu, W.-L.; Lu, L.-J.; Huang, X.-F.; Shangguan, H.-D.; Wei, Z.-Q. An automatic calibration framework based on the InfoWorks ICM model: The effect of multiple objectives during multiple water pollutant modeling. *Environ. Sci. Pollut. Res.* **2021**, *28*, 31814–31830. [[CrossRef](#)] [[PubMed](#)]
- InfoWorks ICM, Version 3.0; Innovyze: Wallingford, UK, 2012.
- HEC-RAS River Analysis System, Version 5.0. 2D Modeling User's Manual. Hydrologic Engineering Center: Davis, CA, USA, 2016.
- Xu, Z.-X.; Cheng, T.; Hong, S.-Y.; Wang, L.-X. Review on applications of remote sensing in urban flood modeling. *Chin. Sci. Bull.* **2018**, *63*, 2156–2166. [[CrossRef](#)]
- Qi, L.; Li, J.; Wang, Y.; Gao, X.-B. Urban observation: Integration of remote sensing and social media data. *IEEE J. Sel. Top. Appl. Earth Obs. Remote Sens.* **2019**, *12*, 4252–4264. [[CrossRef](#)]

19. Teng, J.; Jakeman, A.J.; Vaze, J.; Croke, B.F.W.; Dutta, D.; Kim, S. Flood inundation modelling: A review of methods, recent advances and uncertainty analysis. *Environ. Model. Softw.* **2017**, *90*, 201–216. [[CrossRef](#)]
20. Abdulkareem, J.H.; Pradhan, B.; Sulaiman, W.N.A.; Jamil, N.R. Review of studies on hydrological modelling in Malaysia. *Model. Earth Syst. Environ.* **2018**, *4*, 1577–1605. [[CrossRef](#)]
21. Qi, W.-C.; Ma, C.; Xu, H.-S.; Chen, Z.-F.; Zhao, K.; Han, H. A review on applications of urban flood models in flood mitigation strategies. *Nat. Hazards* **2021**, *108*, 31–62. [[CrossRef](#)]
22. Fan, Y.-Y.; Ao, T.-Q.; Yu, H.-J.; Huang, G.-R.; Li, X.-D. A Coupled 1D-2D hydrodynamic model for urban flood inundation. *Adv. Meteorol.* **2017**, *2017*, 1–12. [[CrossRef](#)]
23. Salvadore, E.; Bronders, J.; Batelaan, O. Hydrological modelling of urbanized catchments: A review and future directions. *J. Hydrol.* **2015**, *529*, 62–81. [[CrossRef](#)]
24. Li, X.-L.; Wang, E.-J.; Zhao, J.; Cheng, M.-G.; Fan, Z.-Q. Waterlogging modeling and simulating for urban crisis management wargaming system. In Proceedings of the 33rd Chinese Control Conference, Nanjing, China, 28 July 2014; pp. 6375–6381.
25. Zhao, L.-L.; Liu, C.-M.; Sobkowiak, L.; Wu, X.-X.; Liu, J.-F. A review of underlying surface parameterization methods in hydrologic models. *J. Geogr. Sci.* **2019**, *29*, 1039–1060. [[CrossRef](#)]
26. Zou, Y.-J. Discussion on urban surface runoff model. *Sci. Surv. Mapp.* **2013**, *38*, 5.
27. Ren, B.-Z.; Deng, R.-J. Analyses of properties and calculation methods of urban surface rainwater conflux. *China Water Wastewater* **2006**, *22*, 39–42. [[CrossRef](#)]
28. Todini, E. On the convergence properties of the different pipe network algorithms. In Proceedings of the Water Distribution Systems Analysis Symposium, Cincinnati, OH, USA, 27–30 August 2006; pp. 1–16.
29. Song, L.-X.; Xu, Z.-X. Coupled hydrologic-hydrodynamic model for urban rainstorm water logging simulation: Recent advances. *J. Beijing Norm. Univ.* **2019**, *55*, 581. [[CrossRef](#)]
30. Yue, M.-L. Study on Risk Simulation and Early Warning of Urban Rainstorms—A Case Study of Zhengzhou City. Master’s Thesis, North China University of Water Resources and Electric Power, Zhengzhou, China, 2019.
31. Jiang, Y.; Zevenbergen, C.; Ma, Y.-C. Urban pluvial flooding and stormwater management: A contemporary review of China’s challenges and “sponge cities” strategy. *Environ. Sci. Policy* **2018**, *80*, 132–143. [[CrossRef](#)]
32. Pender, G. Briefing: Introducing the flood risk management research consortium. In Proceedings of the Institution of Civil Engineers-Water Management; Thomas Telford Ltd.: London, UK, 2006; Volume 159, pp. 3–8.
33. Jamali, B.; Löwe, R.; Bach, P.M.; Urich, C.; Arnbjerg-Nielsen, K.; Deletic, A. A rapid urban flood inundation and damage assessment model. *J. Hydrol.* **2018**, *564*, 1085–1098. [[CrossRef](#)]
34. Niazi, M.; Nietch, C.; Maghrebi, M.; Jackson, N.; Bennett, B.R.; Tryby, M.; Massoudieh, A. Storm water management model: Performance review and gap analysis. *J. Sustain. Water Built Environ.* **2017**, *3*, 04017002. [[CrossRef](#)] [[PubMed](#)]
35. DHI. *Collection System. User Guide*; Danish Hydraulic Institute: Horsholm, Denmark, 2011.
36. Bisht, D.S.; Chatterjee, C.; Kalakoti, S.; Upadhyay, P.; Sahoo, M.; Panda, A. Modeling urban floods and drainage using SWMM and MIKE URBAN: A case study. *Nat. Hazards* **2016**, *84*, 749–776. [[CrossRef](#)]
37. Sidek, L.M.; Jaafar, A.S.; Majid, W.H.A.W.A.; Basri, H.; Marufuzzaman, M.; Fared, M.M.; Moon, W.C. High-resolution hydrological-hydraulic modeling of urban floods using infoworks ICM. *Sustainability* **2021**, *13*, 10259. [[CrossRef](#)]
38. Verma, A.K.; Jha, M.K.; Mahana, R.K. Evaluation of HEC-HMS and WEPP for simulating watershed runoff using remote sensing and geographical information system. *Paddy Water Environ.* **2010**, *8*, 131–144. [[CrossRef](#)]
39. Guidolin, M.; Chen, A.S.; Ghimire, B.; Keedwell, E.C.; Djordjević, S.; Savić, D.A. A weighted cellular automata 2D inundation model for rapid flood analysis. *Environ. Model. Softw.* **2016**, *84*, 378–394. [[CrossRef](#)]
40. Feng, C.-H.; Zhang, N.; Habiyakare, T.; Yan, Y.-N.; Zhang, H. Prospects of eco-hydrological model for sponge city construction. *Ecosyst. Health Sustain.* **2021**, *7*, 1994885. [[CrossRef](#)]
41. Jamali, B.; Bach, P.M.; Cunningham, L.; Deletic, A. A cellular automata fast flood evaluation (CA-Ff'e) model. *Water Resour. Res.* **2019**, *55*, 4936–4953. [[CrossRef](#)]
42. Feng, C.-H. Eco-Hydrological Effects of Urban Landscape Spatial Pattern Change and Simulation. Ph.D. Thesis, University of Chinese Academy of Sciences, Beijing, China, 2022.
43. Agudelo-Otálora, L.M.; Moscoso-Barrera, W.D.; Paipa-Galeano, L.A.; Mesa-Sciarrotta, C. Comparison of physical models and artificial intelligence for prediction of flood levels. *Tecnol. Cienc. Agua* **2018**, *9*, 209–235. [[CrossRef](#)]
44. Mignot, E.; Li, X.-F.; Dewals, B. Experimental modelling of urban flooding: A review. *J. Hydrol.* **2019**, *568*, 334–342. [[CrossRef](#)]
45. Khac-Tien Nguyen, P.; Hock-Chye Chua, L. The data-driven approach as an operational real-time flood forecasting model. *Hydro. Process* **2012**, *26*, 2878–2893. [[CrossRef](#)]
46. Zhu, Z.-D.; Oberg, N.; Morales, V.M.; Quijano, J.C.; Landry, B.J.; Garcia, M.H. Integrated urban hydrologic and hydraulic modelling in Chicago, Illinois. *Environ. Model. Softw.* **2016**, *77*, 63–70. [[CrossRef](#)]
47. Berkahn, S.; Fuchs, L.; Neuweiler, I. An ensemble neural network model for real-time prediction of urban floods. *J. Hydrol.* **2019**, *575*, 743–754. [[CrossRef](#)]
48. Lin, Q.; Leandro, J.; Wu, W.; Bhola, P.; Disse, M. Prediction of maximum flood inundation extents with resilient backpropagation neural network: Case study of Kulmbach. *Front. Earth Sci.* **2020**, *8*, 1–8. [[CrossRef](#)]
49. Löwe, R.; Böhm, J.; Jensen, D.G.; Leandro, J.; Rasmussen, S.H. U-FLOOD—Topographic deep learning for predicting urban pluvial flood water depth. *J. Hydrol.* **2021**, *603*, 126898. [[CrossRef](#)]

50. Zounemat-Kermani, M.; Matta, E.; Cominola, A.; Xia, X.-L.; Zhang, Q.; Liang, Q.-H.; Hinkelmann, R. Neurocomputing in surface water hydrology and hydraulics: A review of two decades retrospective, current status and future prospects. *J. Hydrol.* **2020**, *588*, 125085. [[CrossRef](#)]
51. Hunter, N.M.; Bates, P.D.; Horritt, M.S.; Wilson, M.D. Simple spatially-distributed models for predicting flood inundation: A review. *Geomorphology* **2007**, *90*, 208–225. [[CrossRef](#)]
52. Chang, D.-L.; Yang, S.-H.; Hsieh, S.-L.; Wang, H.-J.; Yeh, K.-C. Artificial intelligence methodologies applied to prompt pluvial flood estimation and prediction. *Water* **2020**, *12*, 3552. [[CrossRef](#)]
53. Zanchetta, A.; Coulibaly, P. Recent advances in real-time pluvial flash flood forecasting. *Water* **2020**, *12*, 570. [[CrossRef](#)]
54. Wei, M.; She, L.; You, X.-Y. Establishment of urban waterlogging pre-warning system based on coupling RBF-NARX neural networks. *Water Sci. Technol.* **2020**, *82*, 1921–1931. [[CrossRef](#)] [[PubMed](#)]
55. Chapi, K.; Singh, V.; Shirzadi, A.; Shahabi, H.; Bui, D.; Pham, B.; Khosravi, K. A novel hybrid artificial intelligence approach for flood susceptibility assessment. *Environ. Model. Softw.* **2017**, *95*, 229–245. [[CrossRef](#)]
56. Khosravi, K.; Panahi, M.; Golkarian, A.; Keesstra, S.D.; Saco, P.M.; Bui, D.T.; Lee, S. Convolutional neural network approach for spatial prediction of flood hazard at national scale of Iran. *J. Hydrol.* **2020**, *591*, 125552. [[CrossRef](#)]
57. Cheng, J.Y.; Xiang, C.; Ma, Y. AI application on LID stormwater management and urban planning in Guam, USA, and Southern China, PRC. In Proceedings of the International Low Impact Development Conference 2020, American Society of Civil Engineers. Reston, VA, USA, 20–24 July 2020; pp. 188–200.
58. Ke, Q.; Tian, X.; Bricker, J.; Tian, Z.; Guan, G.-H.; Cai, H.; Huang, X.; Yang, H.; Liu, J. Urban pluvial flooding prediction by machine learning approaches—A case study of Shenzhen City, China. *Adv. Water Resour.* **2020**, *145*, 103719. [[CrossRef](#)]
59. Tian, Y.; Xu, Y.-P.; Yang, Z.; Wang, G.; Zhu, Q. Integration of a parsimonious hydrological model with recurrent neural networks for improved streamflow forecasting. *Water* **2018**, *10*, 1655. [[CrossRef](#)]
60. Hou, J.; Zhou, N.; Chen, G.; Huang, M.; Bai, G. Rapid forecasting of urban flood inundation using multiple machine learning models. *Nat. Hazards* **2021**, *108*, 2335–2356. [[CrossRef](#)]
61. Ye, X.-Y.; Wang, S.-H.; Lu, Z.-P.; Song, Y.; Yu, S.-Y. Towards an AI-driven framework for multi-scale urban flood resilience planning and design. *Comput. Urban Sci.* **2021**, *1*, 11. [[CrossRef](#)]
62. Goyal, H.R.; Ghanshala, K.K.; Sharma, S. Post flood management system based on smart IoT devices using AI approach. *Mater. Today Proc.* **2021**, *46*, 10411–10417. [[CrossRef](#)]
63. Chen, Y.; Zhang, D. Integration of knowledge and data in machine learning. *arXiv* **2022**, arXiv:2202.10337.
64. Raissi, M.; Perdikaris, P.; Karniadakis, G.E. Physics-informed neural networks: A deep learning framework for solving forward and inverse problems involving nonlinear partial differential equations. *J. Comput. Phys.* **2019**, *378*, 686–707. [[CrossRef](#)]
65. Bermúdez, M.; Cea, L.; Puertas, J. A rapid flood inundation model for hazard mapping based on least squares support vector machine regression. *J. Flood Risk Manage.* **2019**, *12*, e12522. [[CrossRef](#)]
66. Felsberger, L.; Koutsourelakis, P.S. Physics-constrained, data-driven discovery of coarse-grained dynamics. *arXiv* **2018**, arXiv:1802.03824. [[CrossRef](#)]
67. Chen, Y.; Zhang, D. Physics-constrained deep learning of geomechanical logs. *IEEE Trans. Geosci. Remote Sens.* **2020**, *58*, 5932–5943. [[CrossRef](#)]
68. Guo, J.; Wu, X.-H.; Wei, G. A new economic loss assessment system for urban severe rainfall and flooding disasters based on big data fusion. *Environ. Res.* **2020**, *188*, 109822. [[CrossRef](#)] [[PubMed](#)]
69. Gashaw, T.; Tulu, T.; Argaw, M.; Worqlul, A.W. Modeling the impacts of land use–land cover changes on soil erosion and sediment yield in the Andassa Watershed, Upper Blue Nile Basin, Ethiopia. *Environ. Earth Sci.* **2019**, *78*, 679. [[CrossRef](#)]
70. Farooq, M.; Shafique, M.; Khattak, M.S. Flood hazard assessment and mapping of river swat using HEC-RAS 2D model and high-resolution 12-m TanDEM-X DEM (WorldDEM). *Nat. Hazards* **2019**, *97*, 477–492. [[CrossRef](#)]
71. Ejikeme, J.; Igbokwe, J.; Igbokwe, E.; Aweh, D. Evaluation of horizontal and vertical accuracies of SRTM and ASTER GDEM for topographic and hydrological modeling in Onitsha, South East Nigeria. *Int. J. Innov. Res. Sci. Eng. Technol.* **2017**, *4*, 634–643. [[CrossRef](#)]
72. Anthony, E.J. *Shore Processes and Their Palaeoenvironmental Applications*; Elsevier: Amsterdam, The Netherlands, 2008; ISBN 978-0-444-52733-2.
73. Piégay, H.; Arnaud, F.; Belletti, B.; Bertrand, M.; Bizzi, S.; Carboneau, P.; Dufour, S.; Liébault, F.; Ruiz-Villanueva, V.; Slater, L. Remotely sensed rivers in the Anthropocene: State of the art and prospects. *Earth Surf. Process. Landf.* **2020**, *45*, 157–188. [[CrossRef](#)]
74. Maitre, D.C.L.; Kotzee, I.M.; O'Farrell, P.J. Impacts of land-cover change on the water flow regulation ecosystem service: Invasive alien plants, fire and their policy implications. *Land Use Policy* **2014**, *36*, 171–181. [[CrossRef](#)]
75. Zhang, N.; Luo, Y.-J.; Chen, X.-Y.; Li, Q.; Jing, Y.-C.; Wang, X.; Feng, C.-H. Understanding the effects of composition and configuration of land covers on surface runoff in a highly urbanized area. *Ecol. Eng.* **2018**, *125*, 11–25. [[CrossRef](#)]
76. Huang, F.; Zhang, Y.; Zhang, D.; Chen, X. Environmental groundwater depth for groundwater-dependent terrestrial ecosystems in arid/semiarid regions: A review. *Int. J. Environ. Res. Public Health* **2019**, *16*, 763. [[CrossRef](#)]
77. Deng, J.S.; Wang, K.; Hong, Y.; Qi, J.G. Spatio-temporal dynamics and evolution of land use change and landscape pattern in response to rapid urbanization. *Landscape Urban Plan* **2009**, *92*, 187–198. [[CrossRef](#)]

78. Bioucas-Dias, J.M.; Plaza, A.; Camps-Valls, G.; Scheunders, P.; Nasrabadi, N.; Chanussot, J. Hyperspectral remote sensing data analysis and future challenges. *IEEE Geosci. Remote Sens. Mag.* **2013**, *1*, 6–36. [[CrossRef](#)]
79. Chen, Y.; Su, W.; Li, J.; Sun, Z. Hierarchical object oriented classification using very high resolution imagery and LIDAR data over urban areas. *Adv. Space Res.* **2009**, *43*, 1101–1110. [[CrossRef](#)]
80. Liu, B.; Zhang, Y.; Chen, T.; Song, Y. Urban impervious surface extraction based on the GF-2 satellite imagery. *Geomat. World* **2017**, *24*, 103–107.
81. Qi, M.; Huang, H.-B.; Liu, L.; Chen, X. Spatial heterogeneity of controlling factors’ impact on urban pluvial flooding in Cincinnati, US. *Appl. Geogr.* **2020**, *125*, 102362. [[CrossRef](#)]
82. Zhang, Y.; Li, L.; Chen, L.-Q.; Liao, Z.-H.; Wang, Y.-C.; Wang, B.-Y.; Yang, X.-Y. A Modified multi-source parallel model for estimating urban surface evapotranspiration based on ASTER thermal infrared data. *Remote Sens.* **2017**, *9*, 1029. [[CrossRef](#)]
83. Njoku, E.G.; Jackson, T.J.; Lakshmi, V.; Chan, T.K.; Nghiem, S.V. Soil moisture retrieval from AMSR-E. *IEEE Trans. Geosci. Remote Sens.* **2003**, *41*, 215–229. [[CrossRef](#)]
84. Zhou, P.; Ding, J.-L.; Wang, F.; Ubul, G.; Zhang, Z.-G. Retrieval methods of soil water content in vegetation covering areas based on multi-source remote sensing data. *J. Remote Sens.* **2010**, *5*, 15. [[CrossRef](#)]
85. Wang, H.; Sun, X.-B.; Yang, L.-K.; Zhao, M.-R.; Lui, P.; Du, W.-B. Aerosol retrieval algorithm based on adaptive land-atmospheric decoupling for polarized remote sensing over land surfaces. *J. Quant. Spectrosc. Radiat. Transf.* **2018**, *219*, 74–84. [[CrossRef](#)]
86. Mu, Q.; Heinsch, F.A.; Zhao, M.; Running, S.W. Development of a global evapotranspiration algorithm based on MODIS and global meteorology data. *Remote Sens. Environ.* **2007**, *111*, 519–536. [[CrossRef](#)]
87. Ma, M.-H.; Wang, H.-X.; Jia, P.-F.; Tang, G.-Q.; Wang, D.-C.; Ma, Z.-Q.; Yan, H.-M. Application of the GPM-IMERG products in flash flood warning: A case study in Yunnan, China. *Remote Sens.* **2020**, *12*, 1954. [[CrossRef](#)]
88. Kidd, C.; Levizzani, V. Status of satellite precipitation retrievals. *Hydrol. Earth Syst. Sci.* **2011**, *15*, 1109–1116. [[CrossRef](#)]
89. Varma, A.K. Measurement of precipitation from satellite radiometers (visible, infrared, and microwave): Physical basis, methods, and limitations. In *Remote Sensing of Aerosols, Clouds, and Precipitation*; Elsevier: Amsterdam, The Netherlands, 2018; pp. 223–248.
90. Kummerow, C.; Giglio, L. A passive microwave technique for estimating rainfall and vertical structure information from space. Part I: Algorithm description. *J. Appl. Meteorol. Clim.* **1994**, *33*, 3–18. [[CrossRef](#)]
91. Cristiano, E.; ten Veldhuis, M.-C.; van de Giesen, N. Spatial and temporal variability of rainfall and their effects on hydrological response in urban areas—A review. *Hydrol. Earth Syst. Sci.* **2017**, *21*, 3859–3878. [[CrossRef](#)]
92. Kazamias, A.-P.; Sapountzis, M.; Lagouvardos, K. Evaluation of GPM-IMERG rainfall estimates at multiple temporal and spatial scales over Greece. *Atmos. Res.* **2022**, *269*, 106014. [[CrossRef](#)]
93. Tegos, A.; Ziogas, A.; Bellos, V.; Tzimas, A. Forensic hydrology: A complete reconstruction of an extreme flood event in data-scarce area. *Hydrology* **2022**, *9*, 93. [[CrossRef](#)]
94. Giannaros, C.; Dafis, S.; Stefanidis, S.; Giannaros, T.M.; Koletsis, I.; Oikonomou, C. Hydrometeorological analysis of a flash flood event in an ungauged mediterranean watershed under an operational forecasting and monitoring context. *Meteorol. Appl.* **2022**, *29*, e2079. [[CrossRef](#)]
95. Salles, L.; Satgé, F.; Roig, H.; Almeida, T.; Olivetti, D.; Ferreira, W. Seasonal effect on spatial and temporal consistency of the new GPM-Based IMERG-v5 and GSMap-v7 satellite precipitation estimates in Brazil’s Central Plateau Region. *Water* **2019**, *11*, 668. [[CrossRef](#)]
96. He, X.-C.; Gao, W.-J.; Wang, R. Impact of urban morphology on the microclimate around elementary schools: A case study from Japan. *Build. Environ.* **2021**, *206*, 108383. [[CrossRef](#)]
97. Tao, L.; Ryu, D.; Western, A.; Boyd, D. A new drought index for soil moisture monitoring based on MPDI-NDVI trapezoid space using MODIS data. *Remote Sens.* **2020**, *13*, 122. [[CrossRef](#)]
98. Hulley, G.C.; Hook, S.J.; Baldridge, A.M. Investigating the effects of soil moisture on thermal infrared land surface temperature and emissivity using satellite retrievals and laboratory measurements. *Remote Sens. Environ.* **2010**, *114*, 1480–1493. [[CrossRef](#)]
99. Kornelsen, K.C.; Coulibaly, P. Advances in soil moisture retrieval from synthetic aperture radar and hydrological applications. *J. Hydrol.* **2013**, *476*, 460–489. [[CrossRef](#)]
100. Yadav, V.P.; Prasad, R.; Bala, R.; Srivastava, P.K. Synergy of vegetation and soil microwave scattering model for leaf area index retrieval using C-band sentinel-1A satellite data. *IEEE Geosci. Remote Sens. Lett.* **2020**, *19*, 1–5. [[CrossRef](#)]
101. Shulin, C.; Yuanbo, L.; Zuomin, W. Satellite retrieval of soil moisture: An overview. *Advances Earth Sci.* **2012**, *1192–1203*. [[CrossRef](#)]
102. McGinnis, D.; Rango, A. Earth resources satellite systems for flood monitoring. *Geophys. Res. Lett.* **1975**, *2*, 132–135. [[CrossRef](#)]
103. Giustarini, L.; Matgen, P.; Hostache, R.; Montanari, M.; Plaza, D.; Pauwels, V.R.N.; Pfister, L.; Hoffmann, L.; Savenije, H.H.G. Assimilating SAR-derived water level data into a hydraulic model: A case study. *Hydrol. Earth Syst. Sci.* **2011**, *15*, 2349–2365. [[CrossRef](#)]
104. Brakenridge, R.; Anderson, E. Modis-based flood detection, mapping and measurement: The potential for operational hydrological applications. In *Nato Science Series: IV: Earth and Environmental Sciences*; Springer: Berlin/Heidelberg, Germany, 2006; pp. 1–12. [[CrossRef](#)]
105. Gao, W.; Shen, Q.; Zhou, Y.-H.; Li, X. Analysis of flood inundation in ungauged basins based on multi-source remote sensing data. *Environ. Monit. Assess.* **2018**, *190*, 129. [[CrossRef](#)]

106. Brakenridge, G.R.; Nghiem, S.V.; Anderson, E.; Mic, R. Orbital microwave measurement of river discharge and ice status. *Water Resour. Res.* **2007**, *43*. [[CrossRef](#)]
107. Rees, W.G. *Physical Principles of Remote Sensing*; Cambridge University Press: Cambridge, UK, 2013; ISBN 978-1-107-00473-3.
108. Mason, D.C.; Giustarini, L.; Garcia-Pintado, J.; Cloke, H.L. Detection of flooded urban areas in high resolution synthetic aperture radar images using double scattering. *Int. J. Appl. Earth Obs. Geoinf.* **2014**, *28*, 150–159. [[CrossRef](#)]
109. Lin, Y.N.; Yun, S.-H.; Bhardwaj, A.; Hill, E.M. Urban flood detection with sentinel-1 multi-temporal Synthetic Aperture Radar (SAR) observations in a Bayesian framework: A case study for Hurricane Matthew. *Remote Sens.* **2019**, *11*, 1778. [[CrossRef](#)]
110. Bhatt, C.; Thakur, P.K.; Singh, D.; Chauhan, P.; Pandey, A.; Roy, A. Application of active space-borne microwave remote sensing in flood hazard management. In *Geospatial Technologies for Land and Water Resources Management*; Springer: Berlin/Heidelberg, Germany, 2022; pp. 457–482.
111. Zhu, Z.J.; Jiang, A.Z.; Lai, J.; Xiang, Y.; Baird, B.; McBean, E. Towards efficient use of an unmanned aerial vehicle for urban flood monitoring. *J. Water Manag. Model.* **2017**, *26*, C433. [[CrossRef](#)]
112. Colomina, I.; Molina, P. Unmanned aerial systems for photogrammetry and remote sensing: A review. *ISPRS J. Photogramm.* **2014**, *92*, 79–97. [[CrossRef](#)]
113. Feng, Q.; Liu, J.; Gong, J. Urban flood mapping based on unmanned aerial vehicle remote sensing and random forest classifier—A case of Yuyao, China. *Water* **2015**, *7*, 1437–1455. [[CrossRef](#)]
114. Ţerban, G.; Rus, I.; Vele, D.; Brețcan, P.; Alexe, M.; Petrea, D. Flood-prone area delimitation using UAV technology, in the areas hard-to-reach for classic aircrafts: Case study in the North-East of Apuseni Mountains, Transylvania. *Nat. Hazards* **2016**, *82*, 1817–1832. [[CrossRef](#)]
115. Fohringer, J.; Dransch, D.; Kreibich, H.; Schröter, K. Social media as an information source for rapid flood inundation mapping. *Nat. Hazards Earth Syst. Sci.* **2015**, *15*, 2725–2738. [[CrossRef](#)]
116. Sui, D.; Elwood, S.; Goodchild, M. *Crowdsourcing Geographic Knowledge: Volunteered Geographic Information (VGI) in Theory and Practice*; Springer: Berlin/Heidelberg, Germany, 2012; ISBN 978-94-007-4587-5.
117. Filonenko, A.; Wahyono; Hernández, D.C.; Seo, D.; Jo, K.-H. Real-time flood detection for video surveillance. In Proceedings of the IECON 2015—41st Annual Conference of the IEEE Industrial Electronics Society, Yokohama, Japan, 9–12 November 2015; pp. 004082–004085.
118. Li, J.; He, Z.; Plaza, J.; Li, S.-T.; Chen, J.-F.; Wu, H.; Wang, Y.; Liu, Y. Social media: New perspectives to improve remote sensing for emergency response. *Proc. IEEE* **2017**, *105*, 1900–1912. [[CrossRef](#)]
119. Wu, Z.-N.; Shen, Y.-X.; Wang, H.-L.; Wu, M.-M. Quantitative assessment of urban flood disaster vulnerability based on text data: Case study in Zhengzhou. *Water Supply* **2020**, *20*, 408–415. [[CrossRef](#)]
120. Ma, H.-D. Internet of things: Objectives and scientific challenges. *J. Comput. Sci. Technol.* **2011**, *26*, 919–924. [[CrossRef](#)]
121. Poser, K.; Dransch, D. Volunteered geographic information for disaster management with application to rapid flood damage estimation. *Geomatica* **2010**, *64*, 89–98. [[CrossRef](#)]
122. Dhaya, R.; Kanthavel, R. IoT based urban flooding high definition surveillance using concurrent multipath wireless system. *Earth Sci. Inform.* **2022**, *15*, 1407–1416. [[CrossRef](#)]
123. Furht, B.; Villanustre, F. Introduction to big data. In *Big Data Technologies and Applications*; Furht, B., Villanustre, F., Eds.; Springer: Cham, Switzerland, 2016; pp. 3–11. ISBN 978-3-319-44550-2.
124. Gericke, O.J.; du Plessis, J.A. Catchment parameter analysis in flood hydrology using GIS applications. *J. South Afr. Inst. Civ. Eng.* **2012**, *54*, 15–26.
125. Magesh, N.S.; Chandrasekar, N.; Kaliraj, S. A GIS based automated extraction tool for the analysis of basin morphometry. *Bonfring Int. J. Ind. Eng. Manag. Sci.* **2012**, *2*, 4.
126. Anselin, L.; Getis, A. Spatial statistical analysis and geographic information systems. *Ann. Reg. Sci.* **1992**, *26*, 19–33. [[CrossRef](#)]
127. Jing, X.-Y.; Liu, Y.-F.; Wang, Y.-B.; Shen, Y.-Y.; Zhang, S.-F.; Tao, G.-H. Construction of the urban waterlogging monitoring and forecasting system of Harbin City. *J. Catastrophology* **2009**, *24*, 54–57.
128. Wang, Q.-C.; Shou, S.-W.; Zhang, S.-H.; Huo, D.-S.; Zhou, Y.-D. A study on the early warning system for rainstorm Waterlogging in Langfang City of Hebei Province. *J. Arid. Meteorol.* **2013**, *31*, 609–615.
129. Chang, M.-J.; Chang, H.-K.; Chen, Y.-C.; Lin, G.-F.; Chen, P.-A.; Lai, J.-S. A Support vector machine forecasting model for typhoon flood inundation map-ping and early flood warning systems. *Water* **2018**, *10*, 734. [[CrossRef](#)]
130. Van Ackere, S.; Verbeurg, J.; De Sloover, L.; Gautama, S.; De Wulf, A.; De Maeyer, P. A review of the internet of floods: Near real-time detection of a flood event and its impact. *Water* **2019**, *11*, 2275. [[CrossRef](#)]
131. Rong, Y.; Zhang, T.; Zheng, Y.; Hu, C.; Peng, L.; Feng, P. Three-dimensional urban flood inundation simulation based on digital aerial photogrammetry. *J. Hydrol.* **2020**, *584*, 124308. [[CrossRef](#)]
132. Jiménez-Jiménez, S.I.; Ojeda-Bustamante, W.; Ontiveros-Capurata, R.E.; de Marcial-Pablo, M.J. Rapid urban flood damage assessment using high resolution remote sensing data and an object-based approach. *Geomat. Nat. Haz. Risk* **2020**, *11*, 906–927. [[CrossRef](#)]
133. Dungan, J.L.; Perry, J.N.; Dale, M.R.T.; Legendre, P.; Citron-Pousty, S.; Fortin, M.-J.; Jakomulska, A.; Miriti, M.; Rosenberg, M.S. A balanced view of scale in spatial statistical analysis. *Ecography* **2002**, *25*, 626–640. [[CrossRef](#)]
134. McGarigal, K.; Marks, B.J. *FRAGSTATS: Spatial Pattern Analysis Program for Quantifying Landscape Structure*; U.S. Department of Agriculture, Forest Service, Pacific Northwest Research Station: Portland, OR, USA, 1995.

135. Zhang, N.; Zhang, H. Scale variance analysis coupled with Moran's I scalogram to identify hierarchy and characteristic scale. *Int. J. Geogr. Inf. Sci.* **2011**, *25*, 1525–1543. [[CrossRef](#)]
136. Zhang, N. Scale issues in ecology: Concepts of scale and scale analysis. *Acta Ecol. Sin.* **2006**, *26*, 2340–2355.
137. Blöschl, G.; Sivapalan, M. Scale issues in hydrological modelling: A review. *Hydrol. Process.* **1995**, *9*, 251–290. [[CrossRef](#)]
138. Zhang, N. Scale issues in ecology: Upscaling. *Acta Ecol. Sin.* **2007**, *27*(10), 4252–4266.

**Disclaimer/Publisher's Note:** The statements, opinions and data contained in all publications are solely those of the individual author(s) and contributor(s) and not of MDPI and/or the editor(s). MDPI and/or the editor(s) disclaim responsibility for any injury to people or property resulting from any ideas, methods, instructions or products referred to in the content.